Chapter 10

High-Intensity Ultrasound in Pyrometallurgy

The regularities of propagation of high-intensity ultrasound in liquids and melts, as well as related nonlinear phenomena considered in part I of the book, secure an efficient implementation of ultrasonics in some technological processes dealing with molten metals.

This chapter is concerned with the employment of ultrasonics for metal refinement and crystallization, crystal growth, production of as-cast composites, and atomization of melts in the production of powders.

10.1 Ultrasonic Refinement of Melts

Exposure of a liquid to a high-intensity ultrasound reduces the dissolved gas content or, to put it otherwise, degasses the liquid. This effect can also be used for degassing metal melts.

The first papers, concerned with melt degassing, date back to the early 1930s, when a number of degassing methods employing piezoelectric and magnetostrictive transducers had been suggested [1, 2]. A decade later, Esmarch proposed a method for melt degassing that involved the excitation of vibrations by superimposing a permanent magnetic field on the alternating field of an induction furnace (the so-called electrodynamic excitation) [3]. The author experimented with molten aluminum alloy containing 5–7% of magnesium. The melt (8–10 kg) was treated by a 10-kHz ultrasound at 700°C for 30–60 min. The low efficiency of treatment could be accounted for by a low intensity of vibrations imparted to the melt.

The late 1950s saw rapid advances of Russian scientists in the ultrasonic degassing of molten aluminum- and magnesium-based alloys by vibrations directly fed into melts with the aid of sonotrodes [4].

Production of high-quality metals free of abscesses and cavities is a challenging problem in metallurgy. Abscesses and cavities are the result of a drastic decrease in gas solubility in a solidifying melt. It is the excess gas that forms abscesses and cavities. Degassing is expected to reduce the gas content of liquid metals to a level corresponding to gas solubility in solid metals at operation temperatures. Along with conventional methods based on chemical refinement and evacuation, ultrasonic degassing of melts is now coming into industrial use.

Investigations performed by G. I. Eskin on ultrasonic degassing of metal melts made it possible to establish the regularities of ultrasonic degassing of molten aluminum- and magnesium-based alloys, to design devices for ultrasonic treatment of melts simultaneously with shaping and continuous casting, and to develop theory of ultrasonic technology.

Mechanisms of ultrasonic degassing were studied with aluminum (grades A99 and A7), aluminum-magnesium alloys containing up to 8% of Mg, grade AL9 (Al–Si–Mg), AL19 (Al–Cu–Mn), and AL40 (Al–Si–Cu–Mg–Ni–Fe) industrial cast aluminum alloys, grade D1 and D16 (Al–Cu–Mg) wrought alloys, AK6 and AK8 (Al–Cu–Mg–Si) alloys, B95 and 1960 (Al–Zn–Mg–Cu) alloys, as well as grade AMg6 (Al–Mg–Mn) alloy. The use of such a diversity of alloys was dictated by the practical importance of their refinement.

Although being specific for every melt, ultrasonic degassing still obeys some general regularities of degassing. In particular, the efficiency of gas removal from melts parallels the intensity of vibrations. Isochrones of degassing are characterized by the occurrence of special regions (Figure 10.1), which can be attributed to the appearance and development of cavitation. Thus, region I, in which degassing is virtually absent, can be defined as the precavitation region. Region II, in which the efficiency of degassing drastically rises but then becomes steady-state, is the region of treatment conditions corresponding to cavitation.

Cavitation in a melt modifies the ratio of applied and absorbed acoustic powers, which is due to energy expenditure for cavitation and the related 8- to 10-fold drop in the wave resistance of cavitating liquid in response to the change of its state (the presence of cavities affects liquid density and the velocity of ultrasound propagation).

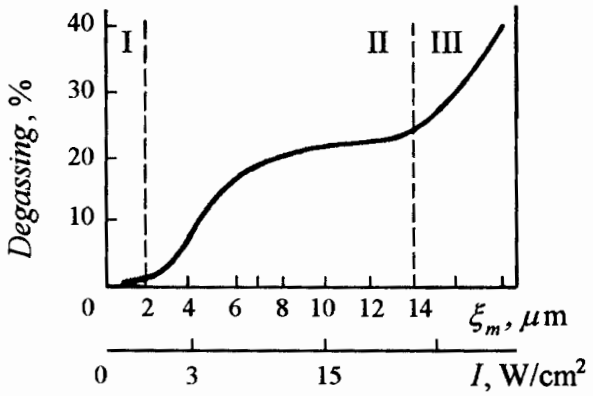

Figure 10.1. Efficiency of degassing of an aluminum-based alloy as a function of the amplitude and intensity of ultrasonic vibrations [5].

With developed cavitation, the efficiency of degassing again rises as the ultrasonic energy fed to the melt increases (region III), which is due to stabilization of the wave resistance of melt at a level corresponding to 0.1–0.2 of its initial value.

Raising the applied acoustic power still further may again lower the efficiency of treatment as the result of a drastic fall in the wave resistance, since cavities will virtually force liquid out of the cavitation region. However, this regime of ultrasonic treatment can hardly be attained, as it is very difficult to feed necessary ultrasonic powers to melts.

The above regularities were proved by numerous experiments with other aluminum- and magnesium-based alloys. The relationship between ultrasound intensity and the efficiency of degassing can be illustrated by the following data: degassing of molten AL9 alloy by vibrations with intensities of 4 and 24 W/cm^2 (all other experimental conditions being identical) requires 24 and 6 min, respectively.

The relationship between the efficiency of degassing and process time is of much practical importance. Figure 10.2 shows the dynamics of hydrogen content in molten AL9 alloy treated at a maximum attainable intensity of ultrasound. It can be seen that the dynamics of hydrogen liberation is virtually independent of its initial concentration. At both initial concentrations, ultrasonic treatment makes it possible to reduce hydrogen content to a minimum level of 0.1 cm^3/100 g alloy. The dynamics of hydrogen evolution allows one to speculate as to the

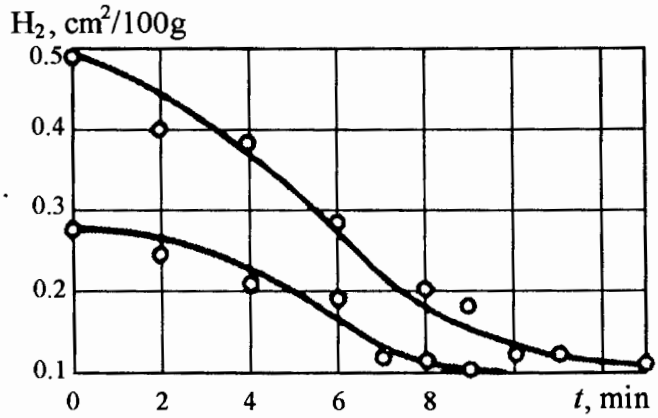

Figure 10.2. Dynamics of hydrogen content in molten Al9 alloys with different initial concentrations of hydrogen [4].

mechanism of gas evolution in an ultrasonic field. Hydrogen concentration in molten AL9 alloy at 720°C is typically 0.45–0.75 cm^3/100 g metal; however, only part of this hydrogen is actually dissolved, the rest being contained in bubbles.

At the initial stage of ultrasonic irradiation, gas bubbles, always occurring in melts, coalesce and emerge to the surface. Further exposure to ultrasound gives rise to new tiny hydrogen bubbles that also coalesce to escape through the melt surface.

Analogous results were obtained in experiments on the degassing of other aluminum-based alloys. At the initial concentration of hydrogen 0.6 cm^3/100 g alloy, the exposure of molten AMg6 alloy (2 kg) to high-intensity vibrations for 20–30 s halves the initial hydrogen content, while irradiation for further 30–40 s reduces it to 0.1 cm^3/100 g.

Analysis of the temperature course of hydrogen evolution curves reveals the existence of optimum degassing temperatures lying, for Al9, between 720 and 760°C. At temperatures below 720°C, the high viscosity of melts prevents bubble coalescence. Above 760°C, the rate of hydrogen liberation becomes comparable with the rate of its absorption by the melt. This is because the solubility of moisture hydrogen in melts increases with temperature.

Radiator material may strongly influence ultrasonic degassing. In particular, titanium radiator was found to be more effective in degassing molten AL9 alloy than niobium or quartz radiators. This might be due to two reasons. First, titanium possesses a higher acoustic qual-

ity than niobium or quartz, since it has a smaller damping coefficient and thus contributes to a lesser extent to energy loss in the vibratory system. At the same input power of transducer, the power fed into a load through niobium radiator is 25% lower than that fed through titanium radiator [4]. Second, transition metals, to which titanium and niobium belong, can efficiently chemisorb hydrogen, nitrogen, and other gases. Disintegration of niobium or titanium radiators results in that some amounts of these metals appear in the melts, where they chemisorb dissolved hydrogen and thus decrease free hydrogen content in melts.

G. I. Eskin assessed the efficiency of ultrasonic degassing with reference to other degassing methods – evacuation and refining of aluminum melts with chlorides.

Reduced pressure may cause desorption of gas molecules from the melt surface and diffusion of new portions of gas to both the melt surface and bubbles in the melt bulk. However, evacuation will not promote the formation of new bubbles. Therefore, for efficient degassing of a bulk melt, it is expedient to combine evacuation with the stimulation of bubble formation. This may be done by ultrasonic irradiation or fluxing.

Figure 10.3 shows the dynamics of hydrogen evolution from molten AL9 alloy caused by evacuation, refining with chlorides, and ultrasonic treatment. It is seen that degassing induced by the addition of salts is insignificant. Thus, the use of salts is mainly owing to their ability to remove solid nonmetallic inclusions from melts. Evacuation is more efficient in degassing than fluxing, but ultrasound works still better. A combined application of ultrasonic treatment and evacuation enhances degassing and diminishes residual concentrations of gases in melts. Such a combined treatment is perhaps the most promising method for production of high-quality ingots of aluminum alloys.

Experiments indicated the feasibility of efficient industrial ultrasonic refining of large-volume melts and melt streams during continuous casting.

In continuous casting, when large melting furnaces and high-performance casting machines are used, it is expedient to perform refining operations in a casting zone. The feeding of ultrasonic vibrations directly to the melt placed in a crystallizer or on the way between a mixer and the crystallizer is more efficient for degassing than their feeding to the crystallizer walls.

The ultrasonic treatment of molten industrial aluminum alloys was found to enhance their purity, castability, the density of as-cast and wrought products, and the quality of ingots and castings.

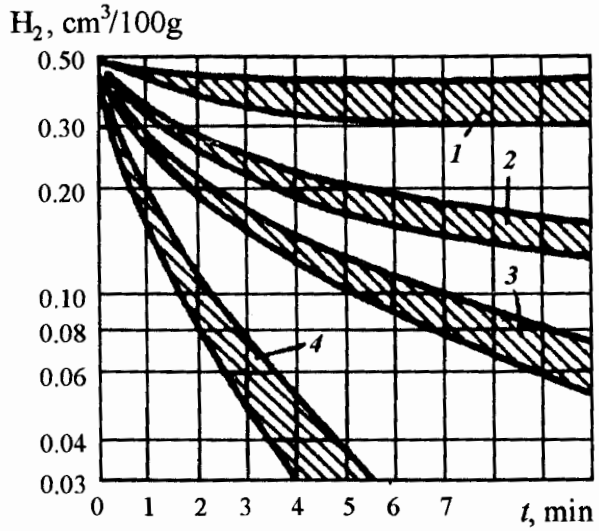

Figure 10.3. Degassing of molten A19 alloy by (*1*) fluxing with zinc chloride, (*2*) evacuation, (*3*) ultrasonic treatment, and (*4*) combined action of ultrasound and evacuation [4].

For illustration, Table 10.1 compares some industrial refining methods employed for a shaped casting of AL4 alloy.

Ultrasonically treated wrought aluminum alloys exhibit an increased density. Table 10.2 summarizes the results of rapid analysis (by the first-bubble method) of hydrogen content in aluminum melts during their continuous casting. It is seen that the efficiency of ultrasonic degassing largely depends on the chemical composition of melts, supplied acoustic power, and the rate of metal casting.

Ingots obtained under ultrasonic degassing exhibited improved mechanical properties at room and elevated temperatures. For instance, the elongation of an AK6 alloy ingot (460 mm in diameter) increased from 5.2 to 8%.

The ultrasonic degassing of molten AMg6 alloy in production of 3- to 10-mm thick sheets made it possible to reduce hydrogen content in rolled intermediate products to 0.25 cm^3/100 g, as well as to avoid their delamination and improve their weldability.

Along with investigation of aluminum-based alloys, attempts are now being made to study the degassing of magnesium-based and other alloys. Thus, analysis of hydrogen content in control and ultrasonically treated molten MA8 alloy showed that even a short-term

Table 10.1 Comparison of various industrial methods for refining grade AL4 alloy [6].

Method	Hydrogen content, $cm^3/100\,g$	Density $\rho \times 10^3$, kg/m^3	VIAM* porosity rating	Mechanical properties	
				σ_B, MPa	δ, %
Control melt	0.35	2.665	4	200	3.8
Refinement by fluxing	0.26	2.660	3–4	225	4.0
Treatment with hexachloroethane	0.30	2.663	2–3	212	4.5
Argon scavenging	0.26	2.667	2–3	233	4.0
Evacuation	0.18	2.681	1–2	228	4.2
Ultrasonic treatment	0.17	2.706	1–2	245	5.1

* Vserossiiskii Institut Aviatsionnykh Materialov (All-Russian Institute of Aviation Materials).

Table 10.2 Efficiency of ultrasonic degassing of continuously cast aluminum alloys [6].

Alloy grade	Crystallizer dimensions, mm	Casting rate, kg/min	Location of ultrasonic radiator	Acoustic power, kW	Hydrogen content, $cm^3/100$ g		Degassing efficiency, %
					Before treatment	After treatment	
AK6	ø250	9.3	In pouring	0.8	0.33	0.18	45
AMg2	ø350	19.7	spout	0.8	0.42	0.30	27
AD1	ø350	13.5	–"–	0.8	0.20	0.16	20
AK6	ø460	15.7	–"–	0.8	0.40	0.21	46
AD1	1040×300	57.5	–"–	0.8	0.25	0.19	24
D16	1480×210	63.0	–"–	0.8	0.38	0.24	37
AMg6	1700×300	82.0	In tap box	6.0	0.60	0.45	25
AMg6	1700×300	82.0	–"–	9.0	0.60	0.40	33
AMg6	1700×300	82.0	–"–	11.0	0.60	0.30	50

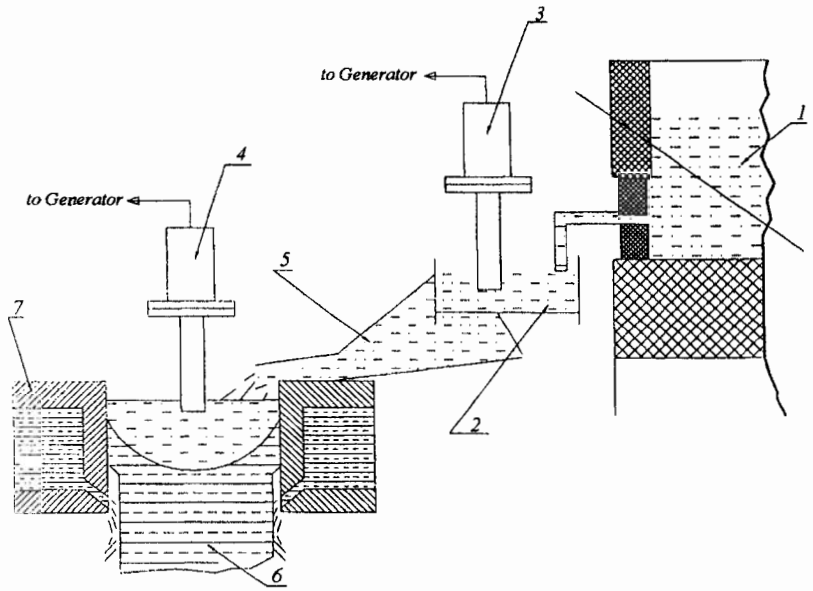

Figure 10.4. Schematic representation of ultrasonic treatment of melt stream [4]: (*1*) furnace with melt, (*2*) intermediate tank, (*3*) ultrasonic transducer for filtration and degassing, (*4*) ultrasonic transducer for structural refinement, (*5*) melt trough, (*6*) crystallizer, (*7*) continuous casting mould.

exposure to ultrasound may reduce hydrogen content of alloys about 2.5-fold [6].

Apart from removing bubbles from melts, ultrasound induces flotation of solid nonmetallic particles and thus lowers their content in aluminum alloys by 10–20%.

The flotation effect of gas-filled bubbles pulsating in an ultrasonic field was first observed by Rosenberg [9] during the ultrasonic refinement studies. Later, Novitskii showed that a pulsating bubble may attract particles irrespective of their nature, density, and wettability [10].

Eskin suggested to use ultrasound not only for the degassing and flotation of solid nonmetallic particles, but also for the fine filtration of melts through multilayer gauze filters [7]. Figure 10.4 shows a combined ultrasonic installation for degassing, filtration (transducer 3), and structural refinement (transducer 4) of continuously cast light alloys. The efficiency of such combined treatment can be assessed by comparing the purity (with respect to nonmetallic inclusions) of large-sized ingots of constructional aluminum-based alloys and the oxide content in filter cake (Table 10.3).

Table 10.3 Efficiency of ultrasound for filtration of molten aluminum-based alloys [5].

Alloy grade	Ingot diameter, mm	Refining method	Number of filtering layers	Hydrogen content of ingot, $cm^3/100\,g$	Oxygen content of filter cake, mass %	Ingots, mm^2/cm^2
D16ch	650	UF	5	0.13	0.09–0.12	0.005
		CF	1	0.16	–	0.025
V95pch	650	UF	2	0.14	0.06–0.10	0.008
		CF	1	0.16	–	0.021
V95pch	830	UF	3	0.18	0.12–0.40	0.005
		CF	1	0.25	–	0.035

Footnote. The mean concentration of oxygen in ingots is 0.01 mass %;
UF stands for fine filtration through a glass cloth (0.6×0.6-mm mesh) in combination with ultrasonic irradiation;
CF stands for conventional filtration through a glass cloth (1.3×1.3-mm mesh).

Thus, experimental data available to date indicate the feasibility of industrial application of ultrasound for melt refining during continuous and shaped castings of light alloys.

10.2 Structural Modification of Solidifying Metals

The vibration of solidifying melts leads to structural refinement of metals and improves their properties.

Sokolov [11, 12] was the first to use ultrasonic treatment of molten low-melting-point metals. However, technical difficulties, associated with the feeding of vibrations to melts, and the lack of suitable ultrasonic generators in the kilohertz range hindered the research along this line.

Since the 1950s, Teumin [13–18], Pogodin-Alekseev [19, 20], Polotskii [21–23], Eskin [4–8, 24, 25], and Abramov [26–32] in the USSR had been carrying out a broad range of research that culminated in the development of ultrasonic equipment for pyrometallurgical applications. Ultrasonic effects on the properties of as-cast materials can be summarized as follows:

(1) Reduction in the mean grain size;

(2) Control of columnar structure and formation of equiaxial grains;

(3) Variation in the distribution of phases in terms of their relative amounts, structural refinement, and mutual geometry;

(4) Improvement of material homogeneity and segregation control;

(5) Uniform distribution of nonmetallic inclusions.

At present, the method of ultrasonic treatment of molten and solidifying metals has been favorably proven by laboratory tests and is finding increasing use in large-scale applications. However, much of the currrent effort is directed toward the elucidation of the mechanism of action of ultrasonic vibrations on solidification (see section 5.1.4), the manufacturing of commercial ultrasonic equipment for metallurgical applications, the development of ultrasonic treatment processes, the evaluation of final structure and properties of products, the assessment of technical and economic aspects of ultrasonic treatment.

This section attempts to address the reader to all these aspects of ultrasonic treatment of solidifying melts. The feeding of ultrasonic vibrations to a solidifying melt is not an easy problem and largely determines the potency of ultrasound in improving the quality of metal castings.

It is known that material tractability is strongly dependent on the ability of ultrasound to penetrate into the melt bulk, in particular, to the front of solidification. The penetrability of ultrasound depends on the method of its feeding and characteristics of casting processes, which should be adapted to ultrasonic technology. These are shaped casting, ingot casting, continuous casting and some refining processes, e.g., vacuum arc remelting (VAR), electroslag remelting (ESR), and electron beam remelting (EBR).

Continuous casting of metals has found a wide use in the past few decades. Continuously cast billets, especially of round or rectangular cross sections, often exhibit coarse-grained structure and axial porosity. During continuous casting, ultrasonic vibrations may be fed to a melt stream, to a liquid metal crater, to a mould, or to a secondary cooling zone.

Special steels, such as nickel-based superalloys and refractory metals, are typically produced in VAR and EBR furnaces, although ESR is also a recommended method of their production. These methods have been developed to control segregation in heavy ingots and ensure

their lower contamination with nonmetallic impurities and gases as compared to ordinary metals. However, all these methods suffer from a disadvantage associated with the formation of a coarse-crystalline columnar structure. This problem can, however, be solved by transmitting vibrations either through the bottom of a solidified ingot or via a consumable electrode.

Figure 10.5,*a* illustrates the transmission of elastic vibrations to a solidifying melt through hole 1 in the mould bottom. Radiating probe 6 is introduced through this hole with a spacing of tenths of a millimeter to avoid molten metal leakage. Figure 10.5,*b* illustrates the method of transmitting vibrations to the upper portion of the melt.

In this method, precautions should be undertaken as to avoid piping or the formation of an upper crust before the melt bulk is completely solidi fied. For this, the cooling of the mould top should be limited. In the top transmission method, ultrasound interacts with a liquid metal, whose volume continuously changes. The top transmission method has found a wide use for degassing aluminum alloys (see section 10.1).

The use of ultrasound in continuous casting is probably most promising. In this case, vibrations may have relatively low intensity, since the amount of metal that solidifies per unit time is constant and rather small. The transmission of vibrations directly to the melt crater is likely the best method of their supply (Figures 10.5,*c* and 10.4); in any event, neither the feeding of vibrations through a mould nor the irradiation of a melt in a tundish are very effective.

The difficulty of creating radiators that could effectively operate for long time periods in molten metals has turned the inventor's mind toward noncontact methods of vibration feeding. One of these is the transmission of vibrations through a billet crust in the secondary cooling zone.

Historically, Seeman and Menzel [36] were the first who applied ultrasonics in continuous casting. They used a 25-kW oscillator, operated at 40 kHz, for driving four magnetostrictive transducers. The system was tested in the casting of 290-mm diameter aluminum rounds. Ultrasonic irradiation was found to refine both macro- and microstructure of ingots and improved their mechanical properties.

Herman [39] described various proprietary designs of equipment used for transmitting ultrasound to the liquid metal crater. Unfortunately, no results of their tests have been reported.

In VAR and ESR, vibrations can be best transmitted from the magnetostrictive transducer through a sonotrode system set to the ingot

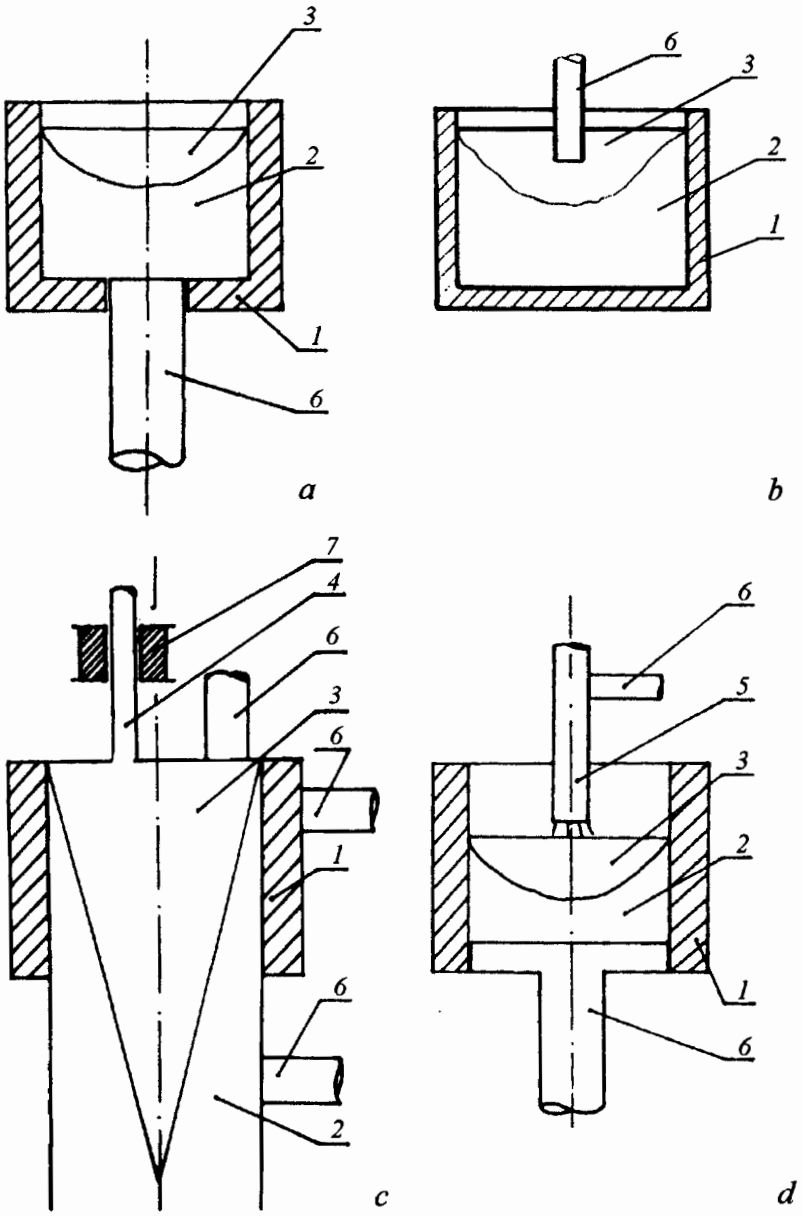

Figure 10.5. Putative schemes of ultrasonic vibration feeding: (*a*) to mould from below, (*b*) to mould from above, (*c*) during continuous casting, (*d*) during remelting. (*1*) Mould (crystallizer), (*2*) solidifying ingot, (*3*) melt, (*4*) metal stream, (*5*) remelting electrode, (*6*) ultrasonic probe, (*7*) ultrasonic funnel.

bottom section and eventually to the solidification zone (Figure 10.5,*d*). Although offering a number of advantages, such as relatively low ultrasound intensity necessary for production of commercial-size ingots and the possibility of using conventional mild-temperature resonators, this method is not free of limitations. As the solidified portion of a solidifying ingot increases, the resonant frequency of the ultrasonic stack-ingot system will vary to disturb the distribution of nodes and antinodes. This may interfere with the normal operation of the transducer and the whole vibratory system and lead to a nonuniform grain refinement in the direction of wave propagation. The result of this will be a gradual transition from fine-grained to coarse-grained structure at half-wave thickness intervals and increased vibrational energy loss during the transmission of vibrations to the solidification front.

Remelting furnaces equipped with ultrasonic stacks were used for processing a number of superalloys, as well as stainless and special steels.

The potentialities of ultrasonic installations with a direct acoustic contact between the melt and resonator are often crippled because of the lack of appropriate materials that would combine high fatigue strength and sufficient resistance to high temperatures, chemical attack, and cavitation.

Because of this, the method of contactless feeding of vibrations to the melt is of much practical interest. In terms of this method, a permanent magnetic field is imposed on the high-frequency field of induction furnace. The resultant electrodynamic forces produce vibrations in the melt [40–44].

In the mid-1930s, Sokolov [11, 12] investigated the effect of ultrasonic vibrations on solidification of pure metals, specifically, tin, zinc, and aluminum. By using piezoelectric transducers operated at frequencies from 600 to 4500 kHz, the author was able to reveal that elastic vibrations can produce a dendrite structure.

Later investigations [23, 45–49] were focused not only on Sn, Z, and Al, but also on Bi, Cd, Sb, and some refractory metals, such as Cr, Ti, Mo, and W. It was found that the grain structure of Cr, Mo, and W was refined as opposed to Ti (Figure 10.6).

Structural changes induced by the solidification of metals in an ultrasonic field can obviously modify their characteristics.

The majority of commercially available pure metals are actually alloys, because of an inevitable impurity contamination. The application of ultrasound to such metals modifies the distribution of phases and affects both grain refinement and zonal and dendritic segregation. As a result, the integral metal properties would change.

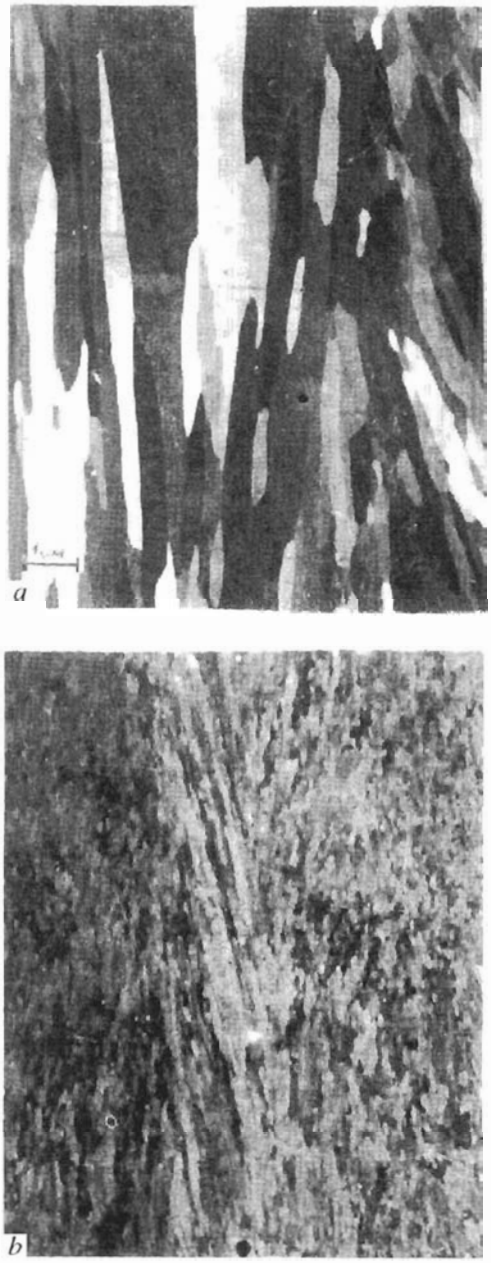

Figure 10.6. Molybdenum microstructure: (*a*) control ingot, (*b*) ultrasonically solidified ingot.

Therefore, to identify the effect of ultrasound on grain refinement, which is the most important metal characteristic, one has to use sufficiently pure metals exhibiting neither segregation nor second phase precipitation.

Several researchers, who approached this problem by using pure Al, Zn, Sn, and Sb, were able to reveal that the strength of as-cast materials can be improved through grain refinement. In particular, Eskin [4] demonstrated that ultrasonic treatment of high-purity Al substantially refined its microstructure (the number of grains per sq. mm increased from 3.1 to 37.5) and thus improved its mechanical properties (tensile strength increased from 5.4 to 7 $kg\,mm^{-2}$, and hardness from HB 17.2 to HB 19.7). The hardening was accompanied by an increase in elongation from 48 to 52%.

Seeman *et al.* [37] showed that an 8-fold increase in the grain size of Sn improved its hardness by 60%. For Zn and Al, the hardness gain was 63 and 80%, respectively.

Grain refinement in Sb was accompanied by a hardness reading rise from HB 34 to HB 52 [47].

Abramov and Gurevich [50] used a 20-kHz ultrasound to vibrate solidifying pure metals with differing crystalline structures: bcc (iron), fcc (nickel and aluminum), hcp (cobalt and zinc), tetragonal (tin), and rhombohedral (bismuth).

It was found that 1-kW power of ultrasound was sufficient to cause grain refinement of Sn and Al (Table 10.4), whereas a 2.5-kW ultrasound elicited the refinement of Fe, Co, Bi, and Zn. However, the results were inconclusive with regard to ultrasonic tractability of metals possessing different lattices.

Structural changes in metals were compared with their properties, viz. hardness (Table 10.4) and tensile strength at −196, 20, and 900°C for Fe, at −196, 20, and 700°C for Co, and at −196 and 20°C for Al (Figure 10.7).

Ultrasonic treatment increased the tensile strength of Fe 1.3-fold at −196°C and slightly improved its ductility. The effect of grain refinement on iron properties was found to be dependent on temperature; at 20°C, the tensile strength and hardness gains were 20 and 6%, respectively, whereas no difference was observed between ultrasonically treated and control specimens at 900°C. At the same time, the difference in ductility increased with temperature, in particular, ultrasonic treatment did not virtually affect elongation at −196°C, but increased it by 10% and 15% at 20 and 900°C, respectively.

sonically

Grain refinement augmented the tensile strength of Al at −196 and 20°C by about 50%. In this case, the hardness tested at room tempera-

Table 10.4 Effect of ultrasonic treatment on the grain size and hardness of metals.

Metal	Transducer input, kW	Grain size, no.	Mean grain diameter, mm	Brinell hardness
Fe	0	−1	0.50	100
	1	−1	0.50	–
	2.5	3	0.12	106
Al	0	1	0.25	16
	1	3	0.12	18
	2.5	4	0.09	19
Co	0	−1	0.50	143
	1	1	0.25	162
	2.5	3	0.12	170
Zn	0	1	0.25	32
	1	1	0.25	–
	2.5	3	0.12	40
Sn	0	−1	0.5	5
	1	2	0.18	6
	2.5	3	0.12	7
Bi	0	−1	0.5	9
	1	−1	0.5	–
	2.5	4	0.09	11

ture increased by 20%. At −196°C, the hardness gain was accompanied by a decrease in elongation. At 20°C, ductility was essentially the same for both ultrasonically irradiated and control aluminum ingots.

Grain refinement in Co improved its strength 2.1 to 2.4 times at all testing temperatures. At room temperature, Co hardness increased by 20%, but its ductility virtually remained unchanged. Ultrasonic treatment raised the hardness of Zn, Bi, and Sn by 22, 25, and 40%, respectively.

Thus, ultrasonically-induced grain refinement of metals leads to considerable changes in their mechanical properties irrespective of the crystal lattice type. Strength is most affected at low temperatures, especially in the case of fcc and hcp metals. With increasing testing temperature, the effect of grain refinement diminishes and virtually disappears in iron (bcc metal). Conversely, the effect of grain refinement on ductility is most profound for bcc metals and grows with increasing temperature.

Figure
alumin

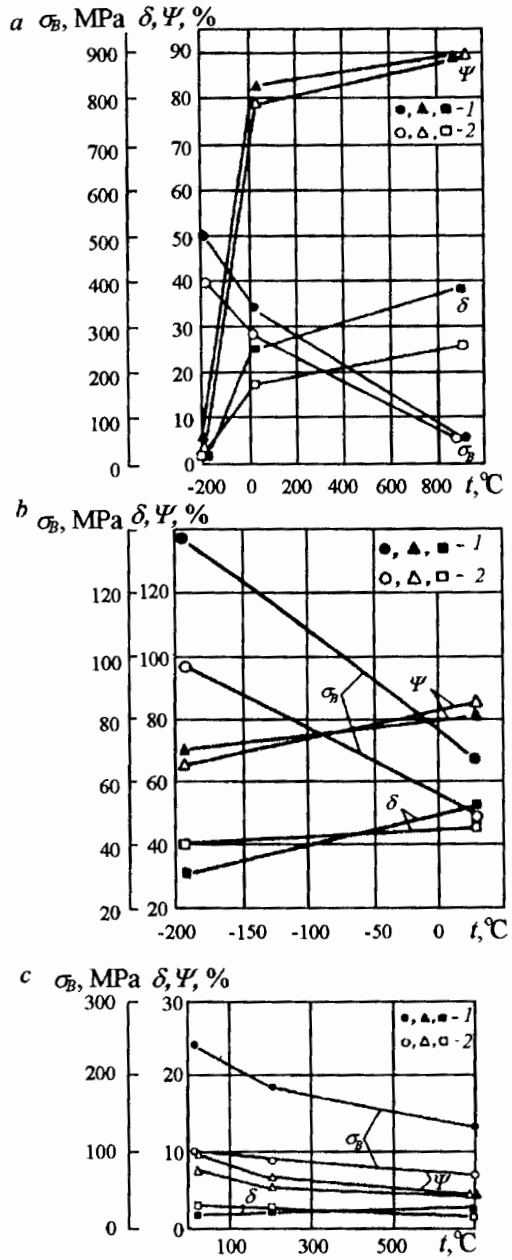

Figure 10.7. Effect of ultrasound on the mechanical properties of (*a*) iron, (*b*) aluminum, and (*c*) cobalt: (*1*) ultrasonically solidified ingots; (*2*) control ingots.

Detailed studies of low-melting alloys based on Sn, Sb, and Bi were performed by Pogodin-Alekseev [19, 20, 51] and Schmid *et al.* [46, 47]. Bi–Pb–Sn–Cd, Bi–Pb–Sn–Cd–Zn, and Bi–Cd low-melting-point alloys typically form dendrite structure during solidification, which allows the effect of ultrasound to be assessed from the dendrite arm reduction. It was found that the formation of dendrite structure is inhibited by ultrasound in all tested ingots, being fully suppressed at a sufficiently high ultrasonic intensity.

The intensity of ultrasonic vibrations in melts was calculated from the crucible vibration amplitude to be about 2 $W\,cm^{-2}$ at 50 Hz and 39 $W\,cm^{-2}$ at 9 kHz. The intensity of 284-kHz vibrations measured calorimetrically was 5 $W\,cm^{-2}$.

These results allowed the authors to conclude that the frequency of vibrations makes only a minor contribution to the changes in ingot structure. This suggestion cannot, however, be considered as unambiguously proven, since a comprehensive investigation of the effect of frequency on solidifying metals is only to be carried out.

Pogodin-Alekseev and coworkers [19, 20, 51] investigated the effect of ultrasound intensity on eutectics in a Pb-Sb alloy and revealed that low-intensity ultrasound produced a nonuniform eutectic structure containing large irregular Sb inclusions, in addition to fine round-shaped particles. With increasing ultrasound intensity, Sb precipitates initially diminished in size and then coalesced.

The authors also studied the structure of excess constituents of Pb–Sb and Zn–Sn alloys during their ultrasonically stimulated solidification and found that even low-intensity vibrations could cause dispersion of the excess phase. Above a certain level of ultrasound intensity, the excess phase tended to coalesce.

Pogodin-Alekseev [52] investigated the effect of audio- and ultrasonic frequences on the structure and properties of babbit and showed that the refinement of β-phase (SnSb) rose with frequency in a range of 20–60 Hz. The increase in the amplitude of low-frequency vibrations from 0.35 to 1.00 mm produced a similar effect. Ultrasonic irradiation reduced crystal size in β-phase and improved the impact properties of babbit more than twofold. The coefficient of friction under incomplete lubrication varied from 0.020 to 0.011 with vibration frequency increase from 20 to 60 Hz. The amplitude of vibrations had a strong effect only at low frequencies.

The ultrasonic treatment of babbit slightly reduced its hardness (from 300 to 230 MPa), augmented its density (from 7.34 to 7.39 $g\,cm^{-3}$), and increased tensile strength from 74 MPa (control specimen) to 90 MPa (ultrasonically treated specimen).

Abramov and Filonenko [53] investigated the effect of ultrasound on solidification of eutectic Sn–Cd, Sn–Pb, and Sb–Pb alloys prepared from high-purity components (max. 5 ppm impurity) and directionally solidified in a 10^{-5} torr vacuum. Ingots were tested for the temperature gradient at the solidification front, the crystal growth rate, overcooling during the growth of colonies, structural spacing, and phase thickness.

A correlation was observed between the structure spacing of regular Sn–Cd and Sn–Pb eutectics or the secondary arm spacing of irregular Sb–Pb eutectic and the crystal growth rate of control specimens (no ultrasound; a temperature gradient of 10 to 20 deg cm^{-1}).

When vibrational power was below a certain level specific for each alloy, the eutectics of Sn–Cd and Sn–Pb alloys retained their regularity under ultrasonic irradiation. Their structural spacing was increased by a factor of 2 to 2.5.

Ultrasonic vibrations with an intensity above the threshold value produced an irregular structure and increased the phase thickness. When the ratio of temperature gradient to crystal growth rate attained max. 10^4 deg s cm^{-2}, the crystals of the Pb-containing solid solution were concentrated at the ingot bottom.

In the hypereutectic Sb–Pb alloy, ultrasound augmented the thickness of precipitating phases (Figure 10.8). These results allowed Abramov and Filonenko to conclude that ultrasound increases the diffusion rate in melts by a factor of 5 to 7.

Pereyaslov and Sapozhnikov [54] examined the effect of ultrasound on the structure, mechanical properties, and corrodability of Pb–Sb alloys with Sb content varying from 0 to 12 wt.%. Solidifying melts were irradiated through the hole in the mould bottom. The displacement amplitude was 6 μm at 20 kHz. Ultrasonic treatment gave rise to a fine equiaxial structure. The addition of 0.1 to 1.0 wt.% Ga refined grains still further. In this case, mechanical properties varied insignificantly, but the resistance of Pb – max. 6% Sb alloys to corrosion in sulfuric acid considerably increased. The corrosion resistance especially increased in alloys that contained 0.2 wt.% Ga.

Eskin and coworkers [4–8, 24, 25] studied the effect of ultrasonic irradiation on aluminum and aluminum-based alloys. In particular, they investigated the solidification of aluminum and binary Al–Cu alloys with different constitution diagrams, as well as commercial castings and wrought alloys.

Ultrasonic irradiation was found to refine the macrostructure of castings. With the copper concentration increasing from 2 to 33%, the efficiency of ultrasonic treatment rose. In this case, the strength of

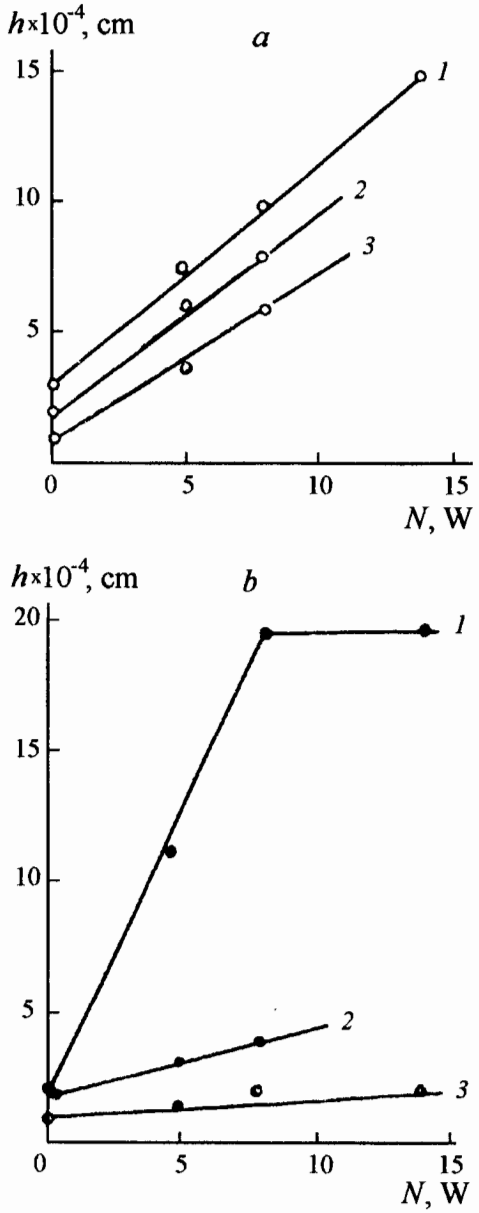

Figure 10.8. Dependence of the high-entropy phase (Sb) thickness on ultrasound intensity: (*a*) $G = 10$ deg/cm; $R = 5 \times 10^{-4}$ (*1*), 6.5×10^{-4} (*2*), and 8.9×10^{-4} cm/s (*3*). (*b*) $G = 20$ deg/cm; $R = 4.87 \times 10^{-4}$ (*1*), 6.87×10^{-4} (*2*), and 8.9×10^{-4} cm/s (*3*).

growing crystals diminished and the solidification temperature range widened.

Structural changes modified the strength and ductility of materials. When melts were cast in a metal mould, the tensile strength of Al alloys containing 2 to 8% Cu increased by 20 to 25% and that of Al alloys containing 12 to 33% Cu remained unchanged. As a result of casting in a ceramic mould, the tensile strength of single-phase and two-phase alloys increased by 50–70% and 20%, respectively. The elongation of all the alloys cast at a high rate remained unchanged and that of the alloys that solidified slowly in a gypsum mould increased by 30 to 100%.

Eskin also studied the effect of ultrasonic vibrations on the formation of intermetallics in Al–Mn, Al–Zr, and Al–Cr alloys.

Microstructure analysis showed that ultrasound, first, enhanced the solidification nuclei formation and, second, suppressed crystal precipitation.

Ultrasonic irradiation considerably improved the tensile properties of alloys, raising tensile strength by 24% (from 170 to 210 MPa), yield strength by 25% (from 140 to 175 MPa), and elongation by 40% (from 12.5 to 17.5%).

Ultrasonic irradiation of peritectically solidifying Al–Zr and Al–Cr alloys produced similar changes. These observations were later confirmed by other researchers [55].

Some investigators performed experiments with Al–Si melts. Thus, Abramov [27] examined a combined effect of ultrasonic irradiation and inoculation on the structure of Al–14% Si alloy. Sodium, as a microadditive, was introduced to the melt at a concentration of 0.1% immediately before pouring.

The macrostructure of untreated cast alloy showed the presence of the large segregates of excess Si crystals against the background of relatively coarse eutectics. By contrast, ultrasonic irradiation and microalloying with Na refined silicon crystals and uniformly distributed them over the ingot.

When inoculation was performed without ultrasonic irradiation, the shape of excess Si crystals changed, but the eutectics structure remained fairly coarse.

Eskin and coworkers [4–8, 24, 25] investigated a number of commercial Al alloys. Like in the case of model alloys, the ultrasonic irradiation of commercial alloys refined their structure and improved their mechanical properties (Table 10.5).

It was also found that ultrasound can substantially suppress zonal segregation of Zr, Ti, Cr, and Mn, i.e., the additives that strongly differ from aluminum in density.

Table 10.5 Effect of ultrasound on the mechanical properties of commercial aluminum-based alloys [4].

Alloy grade	Alloy system	Alloy condition	Ultrasonic treatment	UTS, MPa	Elongation, %	Area reduction, %	Brinell hardness
AL40	Al–Si–Cu–Mg–Ni–Fe	As-cast	No	160	5	–	64
		–"–	Yes	210	6	–	75
		Heat-treated	No	250	3	–	89
		–"–	Yes	330	5	–	96
AL19	Al–Cu–Mn	As-cast	No	270	3	–	–
		–"–	Yes	350	4	–	–
AL20		–"–	No	190	5	6	72
		–"–	Yes	210	11	12	76

Dobatkin and Eskin [5] determined the conditions of continuous casting, under which a dendrite-free grain structure was formed. This type of structure could be observed, if the grain size was smaller than or equal to the size of a dendrite cell produced at a given solidification rate. Cavitation in the melt appeared to be the necessary condition for an as-cast subdendrite structure to develop.

As a result, Dobatkin and Eskin could produce 850-mm diameter cast billets from most commercially available inoculated aluminum alloys with the subdendrite structure. Table 10.6 lists the linear grain sizes of subdendrite and dendrite structures averaged over 5 to 40 billets of several commercial aluminum alloys. In ultrasonically treated ingots, the as-cast structure exhibited a uniform refinement across the section, whereas untreated ingots had a fan-like dendrite structure.

Similar results were obtained for ultrasonically treated Mg alloys [57, 58].

Ultrasonically induced grain refinement and the dendrite-to-subdendrite structural changes increased the ductility of ingots at both room and high testing temperatures (Table 10.7).

Ultrasonic irradiation during a continuous casting of 550 × 160-mm ingots of grade MA2-1 magnesium alloy resulted in a marked grain refinement. Control ingot exhibited a nonuniform structure across its section: 1- to 3-mm equiaxial grains in the core and 5- to 7-mm columnar grains in the transverse direction near larger faces. The columnar zone was 45 mm long.

Table 10.6 Effect of ultrasonically induced cavitation in molten light alloys on the grain refinement of ingots [5].

Alloy system	Alloy grade	Ingot size, m	Inoculant concentration, %		Grain size, μm	
			Zr	Ti	Ultrasound	Control
	1960, 1965, 1963, V96Ts-1	0.06–0.37	0.15	0.04	20–70*	300–1500
Al–Zn–Mg–Cu	V95pch, 7050, 7010, V934	0.06–0.98	0.15	0.04	20–140*	500–200
Al–Cu–Mg	D164, 2024	0.06–0.98	0.15	0.04	20–140*	300–200
Al–Cu–Mn	1201, D20-1	0.07–0.37	0.18	0.06	25–90*	300–120
Al–Mg–Mg	1561	0.37	0.16	0.06	90*	1500
Mg–Al–Zn	MA2-Ipch	0.12 0.55–0.165	0.003	–	50–500	120–400
Mg–Zn–Zr	MA14	0.17	0.1–0.4 0.03	–	60*	190
Mg–Y–Ce–Zr	MDZ-3	0.3×0.1	0.6 0.03	–	60*	300
Mg–Y–Nd–Zn–Zr	VMD-7 VMD-9	0.17	0.14 0.03	–	30*	200

* Subdendrite grain.

Table 10.7 Tensile strength of grade 1960 (Al–Zn–Mg–Cu) alloy under homogenizing conditions [6].

Ingot diameter, mm	Structure type	UTS, MPa	Elongation, %
	Testing at 20°C		
65	Dendrite	226	3.8
	Subdendrite	225	4.0
270	Dendrite	206	2.0
	Subdendrite	207	2.9
	Testing at 400°C		
65	Dendrite	35	98.0
	Subdendrite	37	132.0
270	Dendrite	39	108.0
	Subdendrite	40	122.0

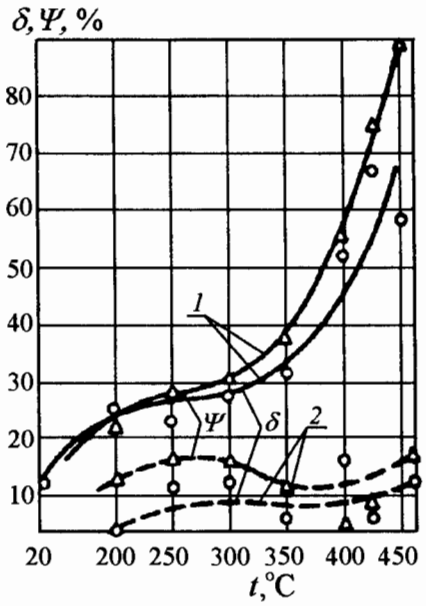

Figure 10.9. Ductility of homogenized grade MA2-1 alloy versus testing temperature [6]: (*1*) ultrasonically solidified ingot; (*2*) control ingot.

Ultrasonic treatment produced 0.3- to 0.5-mm equiaxial grains over the entire billet section and reduced the dendrite cell size. This appreciably improved material ductility, especially in the surface region. The ductility of control ingot was virtually independent of testing temperature, whereas in ultrasonically treated ingot both elongation and area reduction grew with temperature up to 450°C.

Ultrasonic treatment also raised the permissible strain level in metal working processes. The inherent effect of the refined as-cast structure on the quality of worked metals was retained even after relatively high strains. In fact, after the rolling of 150-mm thick cast slabs into 0.8–2.5-mm sheets, the ductility was greater for sheets produced from ultrasonically treated metal (Figure 10.9).

Pogodin-Alekseev [19, 59] studied the effect of elastic vibrations on copper-based alloys, viz. grade Br. OTsS-5-5-5, Br. OTsS-6-6-3, Br B2, Br B5, and BNT bronzes, and evaluated the contribution from displacement amplitude to the structure and properties of ingots produced by shaped and continuous castings.

When vibrations were transmitted directly to cast grade Br. OTsS-5-5-5 alloy, both low- and ultrasonic-frequency irradiation refined their

macro- and microstructure and modified the mechanical properties of the alloy. Low and high frequences augmented the tensile strength of ingots by 20 and 40% and their elongation by 15 and 35%, respectively.

In the case of cast grade Br. OTsS-6-6-3 bronze, ultrasonic vibrations fed to shell moulds were found to modify the structure and properties of castings as well. In particular, tensile strength increased by 34 and 43% as a result of low-frequency and ultrasonic vibrations, respectively. It was also found that irradiated specimens offered better corrosion resistance.

Ultrasonic irradiation of grade BNT bronze increased its elongation and area reduction by 26 and 15%, respectively. Impact strength remained unchanged, while density was slightly increased.

It follows from the literature data that single-phase alloys possess fair ultrasonic tractability. This supposition was verified on a number of Cu–Al, Cu–Sn, and Cu–Zn alloys [29].

The Cu–Al alloys studied contained 1, 5, 7, 9, and 12% Al. The first three (α-alloys) and the last (β-alloy) were single-phase, whereas the alloy with 9% Al contained both α and β phases. All the alloys exhibited a narrow solidification temperature range.

The Cu–Sn alloys studied contained 2, 8.5, 13, and 15% Sn. The first three alloys (α-alloys) were single-phase, and the fourth was two-phase (α, β-alloy). The solidification temperature range was quite narrow for Cu–2% Sn alloy, but extended to 140°C for the alloys containing 8.5 and 15% Sn, and to 175°C for the alloy with 13% Sn.

In the Cu–Zn system, single-phase α-alloys contained 10, 20, and 30% Zn, two-phase α, β-alloy contained 35% Zn, and single-phase β-alloy contained 45% Zn. The solidification temperature range was from 10 to 20°C for all of these alloys.

Ultrasonic input power (1100 W) was kept constant in all tests. The macrograin refinement factor K, i.e. the ratio of the grain sizes of control and irradiated alloys, was taken as a tractability characteristic.

Experiments revealed no essential effect of ultrasound on the tractability of single-phase and two-phase alloys. However, ultrasound increased the tractability of the solid solution-type alloys, as follows from measurements of the grain refinement factor (see Table 10.8).

The micrograins were appreciably refined in solid solution-type alloys. The structure of two-phase alloys became more dispersed.

The Cu–Sn alloys exhibited a much better tractability than Cu–Al and Cu–Zn alloys did. This is probably due to a wider solidification temperature range of the former alloys.

Table 10.8 Ultrasonic tractability taken as the grain refinement factor K of Cu–Al, Cu–Sn, and Cu–Zn alloys.

Al, %	Phases	K	Sn, %	Phases	K	Zn, %	Phases	K
1	α	7	2	α	9	10	α	11
5	α	13	8.5	α	26	20	α	6
7	α	11	13	α	20	30	α	6
9	$\alpha+\beta$	5	15	$\alpha+\beta$	14	35	$\alpha+\beta$	5
12	β	10				45	β	2

Vasin *et al.* [60] investigated the effect of ultrasonic irradiation on the structure and properties of grade OTs10-2 bronze. Ultrasonic vibrations were transmitted through a water-cooled funnel. Casting flow rate and melt temperature were varied.

Under optimal conditions, ultrasonic irradiation led to structural refinement, columnar zone suppression, and controlled porosity. As a result, tensile strength was increased by 35%, yield strength by 20%, elongation by 10%, and hardness by 8 to 12%.

There have been a few studies of the efficiency of ultrasonic treatment of various ferrite, austenite, and carbide steels, plain-carbon and low-alloy steels, boron-containing steels, and cast irons. These studies were performed with grade St20, St30, St40, St50, U8, U10, 17MnSi, 30CrMnSi, 35CrMo, 45Mn2, 55Si2 [27], and ShCr15 [61] plain-carbon and low-alloy steels. The selection of the above metals was primarily motivated by their practical importance and the necessity to improve their mechanical properties and workability.

Vibrations were transmitted to a solidifying metal through the hole in the mould bottom, or during continuous casting (grade ShCr15 ball bearing steel), or during VAR (grade U10).

It was found that the efficiency of ultrasonic treatment of plain-carbon steels increased with carbon content, so that hypoeutectoid steels with carbon contents of less than 0.4% exhibited a relatively low ultrasonic treatability. At the same time, ultrasound produced a substantial grain refinement in grade U8 and U10 steels.

Such a dependence of ultrasonic treatment efficiency on the carbon content of steels basically follows from the iron-carbon phase diagram, i.e. from the solidification temperature range width, and the strength of growing crystals.

Significant structural modifications obviously exerted effect on the mechanical properties of steels (Table 10.9).

Table 10.9 Effect of ultrasound on the mechanical properties of plain-carbon and low-alloy steels.

Steel grade	Ultrasonic treatment	UTS, MPa	YS, MPa	Elongation, %	Reduction of area, %	U-notch Charpy toughness, MJ/m^2	Vickers hardness
St40	No	620	360	12	16	0.40	155
	No*	750	670	8	9	0.30	190
	Yes	710	450	8	10	0.30	175
	Yes*	810	700	7	8	0.30	246
St50	No	490	–	10	15	0.15	–
	Yes	630	–	18	28	0.28	–
U10	No	480	400	2	5	–	242
	Yes	850	410	3	9	–	254
40CrNi	No	880	560	9	14	–	–
	Yes	900	570	12	25	–	–
SiCrNiMo**	No	2380	2300	4	40	0.38	–
	Yes	2530	2430	3	50	0.57	–

* Additionally inoculated with 0.1% Ti.

** Thermomechanically treated, i.e. rolled at 525°C with a reduction of 60 to 78%, quenched, and tempered at 200°C for 1 h.

Ultrasonic irradiation of St50 steel improved its tensile performance at room temperature. The strength and ductility of this steel increased by 20–30 and 30%, respectively.

Ultrasonic irradiation of grade U10 steel increased its tensile strength, elongation, and area reduction by about 75, 30, and 60%, respectively; hardness and yield strength did not virtually change.

Experiments with grade ShCr15 ball bearing steel were aimed at elucidating the effect of ultrasound on ingot homogeneity, structure banding, dendrite segregation, and the shape and distribution of non-metallic inclusions. Comparative structural analysis showed that ultrasonically treated ingots possessed much lower carbide segregation, with a finer and more uniformly distributed carbide phase in comparison with control ingots (Figure 10.10).

Some works [62–64] were devoted to the effect of ultrasound on the structure and properties of ferrite steels and alloys with the bcc lattice, i.e. grades Cr13, Cr18, Cr25Ti, Cr27, Si3, Si6 (with carbon concentrations of 0.02 and 0.1%), Al14 and Al16.

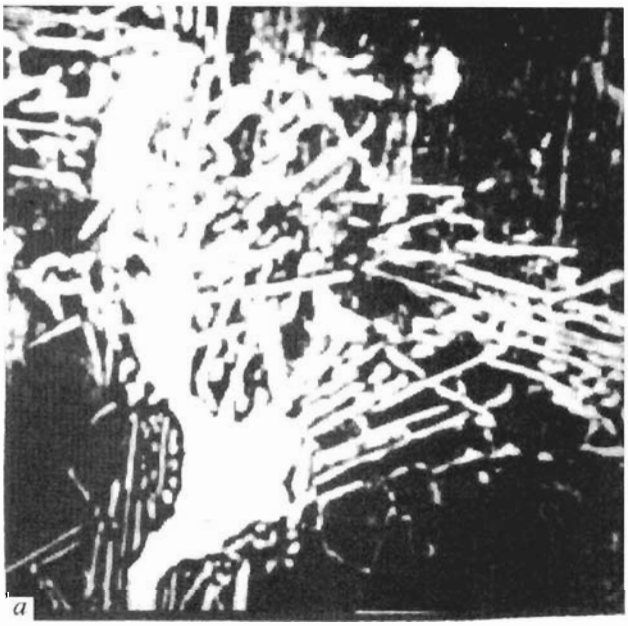

Figure 10.10. Carbide phase segregation in (*a*) control and (*b*) ultrasonically solidified ShCr15 steel ingots (×500 magnification).

Table 10.10 Effect of ultrasound on the mechanical properties of ferritic steels.

Steel grade	Condition	Testing temperature, °C	Ultrasonic treatment	UTS, MPa	YS 0.2%, MPa	Elongation, %	Area reduction, %	Torsional shear
Cr13	As-cast	−196	No	230	–	1	4	–
		−196	Yes	290	–	2	6	–
		20	No	170	–	5	14	–
		20	Yes	20	–	8	30	–
Cr25Ti	As-cast	20	No	330	250	12	15	–
			Yes	460	360	14	18	–
		900	No	30	25	28	51	–
			Yes	35	25	68	90	–
		1100	No	6	–	53	77	25
			Yes	9	7	110	90	45
		1200	No	3	–	72	82	25
			Yes	6	3	80	90	40
Cr27	As-cast	20	No	450	320	6	6	50
		20	Yes	530	350	20	44	89
	As-heat treated	20	No	480	320	14	29	70

Ferrite steels and alloys showed a rather high ultrasonic treatability. The ultrasonic treatment of these materials suppressed their columnar structure, refined macro- and micrograins, and improved ingot homogeneity.

Changes in the ingot structure enhanced the strength and ductility of tensile specimens at room temperature and in metal-working temperature ranges (Table 10.10). Ultrasound also improved impact toughness and permissible reductions during the rolling of V-shaped specimens. Similar results were obtained for Fe–Si (grades Si3 and Si6) and Fe–Al (grades Al4 and Al16) alloys.

Ultrasonic irradiation increased the tensile strength, elongation, and area reduction of as-cast materials 1.2–1.6 times, 3–5 times, and 3–10 times, respectively. After subsequent thermal treatment and working, differences in the properties of control and ultrasonically treated ingots, even though being somewhat diminished, remained rather great.

Effect of ultrasound on the structure and properties of austenitic alloys was studied using Cr18Ni9, Cr25Ni20, Cr20Ni20Mo3, CrNi35WTiAl, and Mn12 steels [62–64].

Table 10.11 Effect of ultrasound on the mechanical properties of austenitic steels.

Steel grade	Testing temperature, °C	Ultrasonic treatment	UTS, MPa	Elongation, %	Area reduction, %	U-notch Charpy toughness, MJ/m^2
12Cr18Ni9	20	No	480	31	65	–
		Yes	520	45	75	–
Cr25Ni20	20	No	460	25	44	1.3
		Yes	560	32	71	1.8
	950	No	80	16	25	0.9
		Yes	70	26	32	1.2
Cr20Ni20Mo3	20	No	490	42	40	–
		Yes	550	54	68	–
	900	No	140	22	18	1.1
		Yes	170	28	26	1.7
	1100	No	50	12	7	0.3
		Yes	50	15	12	0.4

To be efficient in the treatment of austenitic steels, ultrasound should have higher intensity than in the case of ferritic steels.

Structural changes in austenitic steels were responsible for the differences in the mechanical properties of control and ultrasonically treated ingots (Table 10.11).

Grade W18 tool steel was used to elucidate the effect of ultrasound on segregation in carbide steels [30]. Ultrasonically treated ingots exhibited the refinement of macro- and fracture structures, as well as the modification of their microstructures. Moreover, carbide eutectics were also refined (Figure 10.11). Of particular interest is the fact that ultrasonically induced structural changes persisted after the complete processing cycle of W18 steel (forging at 1100°C, annealing at 800°C, oil quenching from 1280°C, and tempering at 560°C for 1 h). The extent of carbide segregation in ultrasonically treated steel (2.5) was substantially lower than that in control ingot (4.5).

The effect of ultrasound on the structure and mechanical properties of iron castings was studied by Gorev *et al.* [65–67] and Levi *et al.* [68–72]. Ultrasonic treatment drastically refined spherical graphite precipitates in iron castings irrespective of their carbon and silicon contents. As a result, the white iron structure of low-carbon, low-silicon alloys transformed into ferritic.

Figure 1
trol ingot

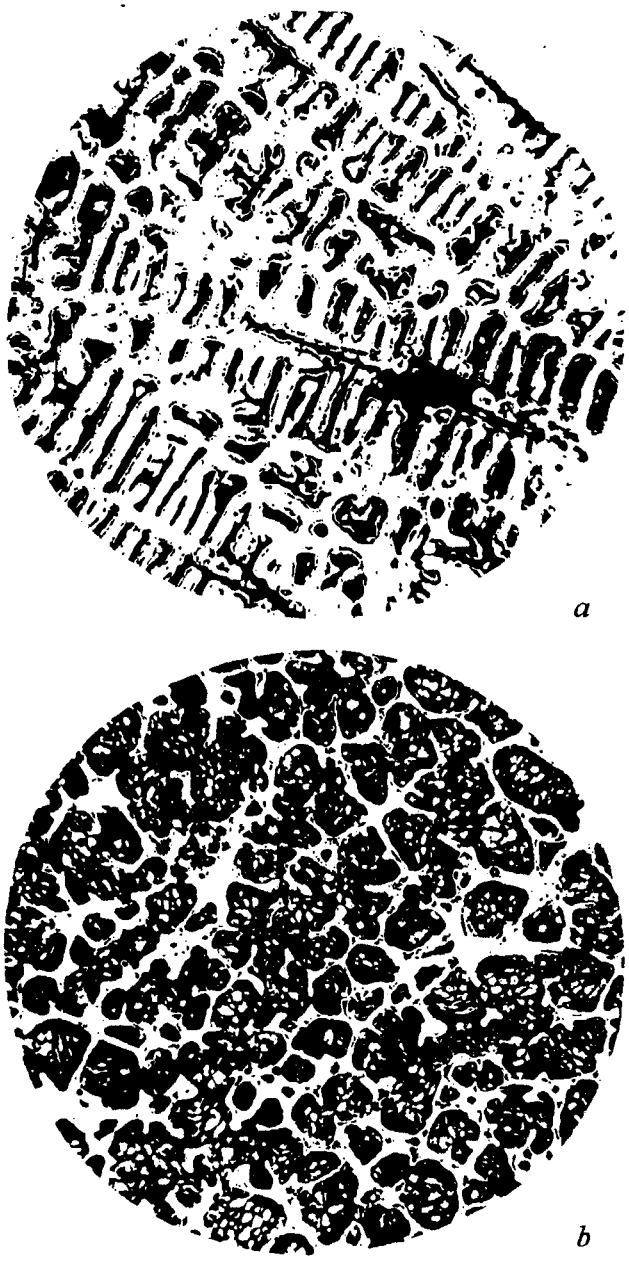

Figure 10.11. Microstructure of grade R18 steel (×100 magnification): (*a*) control ingot, (*b*) ultrasonically solidified ingot.

Abramov [27, 73] investigated the effect of ultrasound on the structure and properties of such boron-containing steels as Cr18Ni15B2, Cr18Ni10B2, Cr17B2, and Cr18Ni6Mn9B2, which form a brittle phase when solidified.

Steels with a high boron content are usually poorly workable. The objective of ultrasonic treatment was to improve the workability of boron-containing steels and to elucidate their suitability for manufacturing tubular products and strips.

It should be noted that ultrasonic treatment caused structural refinement of basic (i.e., free of boron) hypereutectic steels of grades Cr18Ni10, Cr18Ni15, Cr18Ni6Mn9, and Cr17 (Figure 10.12).

On the other hand, microstructure analysis of grade Cr18Ni15B3 boron-containing hypereutectic steel indicated the occurrence of a large amount of boride phase that was highly refined under the action of ultrasound (Figure 10.13).

Matrix microstructure was also modified by ultrasound, namely, eutectics were refined as compared to control ingot.

Ultrasonic treatment largely modified the mechanical properties of boride steels (Table 10.12). Tests were carried out in two temperature ranges: 20–600 (service temperatures) and 900–1150°C (working temperatures).

Investigation of the effect of ultrasonic irradiation on the structure and properties of precipitation-hardened refractory Ni-based superalloys is of much practical importance because of their weak ductility and narrow temperature range of deformation. In this connection, it was of interest to examine a method that could improve the workability of these alloys at technological temperatures without impairing their service properties. An enhanced ductility could ensure a substantial saving of the cost of rolled products and appreciably increase their quality by obtaining more efficient billet profiles and reducing the ratio of surface-defective billets.

Ultrasonic treatment was carried out in the process of vacuum arc remelting with vibrations transmitted through the ingot bottom. To find the optimum conditions of remelting and ultrasonic treatment, it was necessary to match melting rates with the intensity of ultrasonic vibrations. The efficiency of ultrasound was defined as the refinement of ingot microstructure. Remelting rate was varied from 0.015 to 0.033 kg/s by changing the electric parameters of remelting.

Macrostructure analysis of ingots of refractory, nickel-based alloys Cr20Ni80, CrNi77TiAlB, CrNi56WMoCoAl, and CrNi51WMoTiAlCoVB showed that they are ultrasonically workable. Indeed, ultrasonic treat-

Figure
control

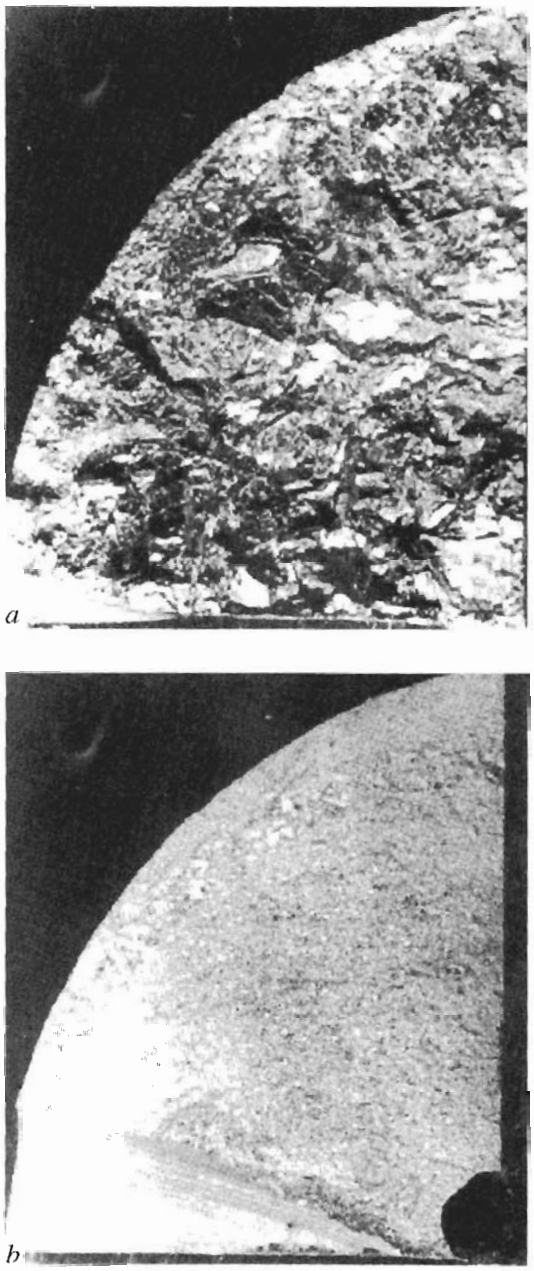

Figure 10.12. Fracture of grade Cr18Ni15B3 boron steel (×8 magnification): (*a*) control ingot, (*b*) ultrasonically solidified ingot.

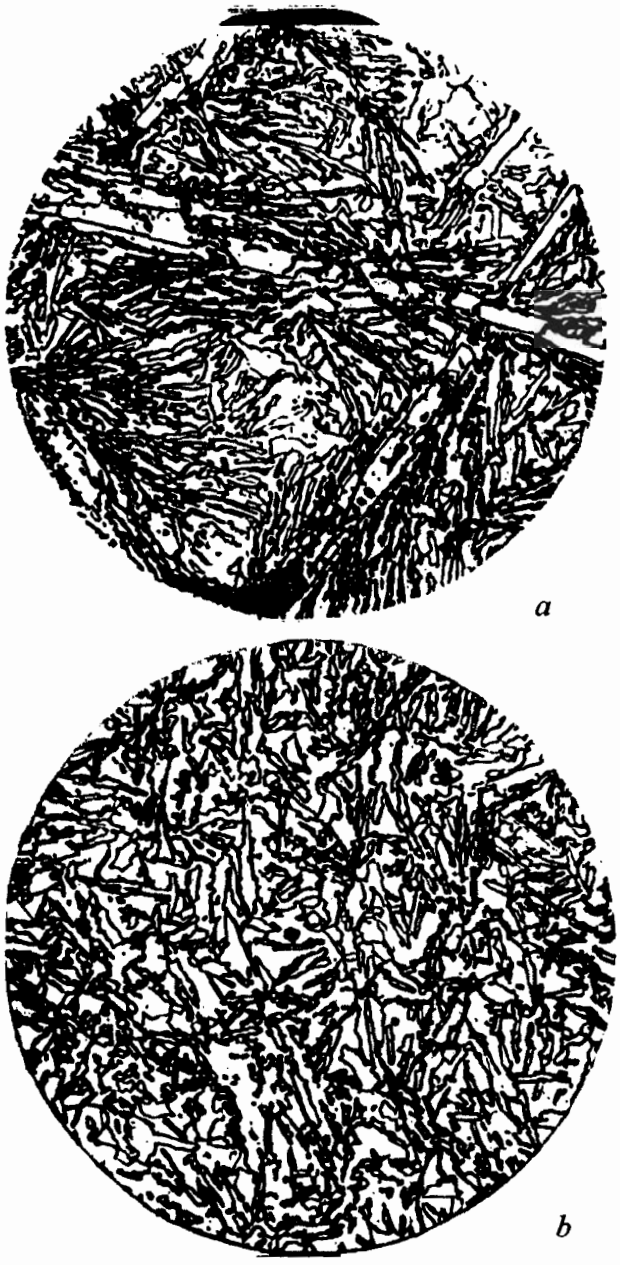

Figure 10.13. Microstructure of Cr18Ni15B3 steel (×100 magnification): (*a*) control ingot, (*b*) ultrasonically solidified ingot.

Table 10.12 Effect of ultrasound on the mechanical properties of as-cast boron steels.

Steel grade	Boron content, %	Testing temperature, °C	Ultrasonic treatment	Tensile strength, MPa	Elongation, %	Area reduction, %	Max. rolling deformation, %
Cr18Ni15B2	2.4	550	No	250	–	–	–
			Yes	330	–	–	–
		1100	No	20	23	19	–
			Yes	20	23	32	–
Cr18Ni15B3	2.8	600	No	260	–	–	–
			Yes	400	–	–	–
		1100	No	70	14	14	16
			Yes	60	34	41	28
Cr18Ni10B3	3.2	350	No	100	0	0	–
			Yes	280	1	1.5	–
		1150	No	10	4	1	6
			Yes	25	8	3.6	37
Cr18Ni6Mn9B3	3.4	350	No	90	0	0	–
			Yes	260	0	0	–
		1150	No	19	3.5	0	4
			Yes	32	9.5	11	20

ment at optimal remelting rates and vibration intensities brought about the removal of the columnar structure of ingots and produced a sufficient refinement of their macrostructure over the entire ingot bulk.

The technological ductility of ingots, produced in a vacuum arc furnace conventionally and ultrasonically, was assessed from tensile and torsional strengths and toughness measured at temperatures of hot machining (1000 to 1200°C). The method of V-shaped specimen rolling was also used, which allowed a more complete estimation of metal behavior during hot plastic deformation (Table 10.13).

Analysis of experimental data indicated that the application of ultrasonic vibrations during remelting in a vacuum arc furnace improved the ductility of refractory alloys at temperatures of hot machining.

Ultrasonic treatment improved the extrusion workability of alloys CrNi51WMoTiAlCoVB and CrNi56WMoCoAl, so that they could be extruded in a wider temperature range.

Table 10.13 Maximum permissible rolling stress of V-shaped superalloy specimens.

Superalloy	Ultrasonic treatment	Maximum rolling stress (MPa) at testing temperature (°C)					
		900	1000	1050	1100	1150	1200
CrNi77TiAlB	No	48	44	43	44	43	45
	Yes	51	48	50	51	57	47
CrNi56MoWCoAl	No	–	30	33	44	52	42
	Yes	–	34	37	54	56	57
CrNi51WMoTiAlCoVB	Yes	–	6	12	16	6	3
	No	–	11	14	19	14	9

Micrograins were found to be smaller in ultrasonically treated alloys, the degree of refinement being greater for CrNi51WMoTiAlCoVB. For comparison, the micrograin counts were 0 and 2–3 for control and ultrasonically treated CrNi51WMoTiAlCoVB ingots and 0–1 and 1–2 for control and irradiated CrNi56WMoCoAl ingots, respectively.

As-worked speciments of CrNi56WMoCoAl and CrNi51WMoTiAlCoVB alloys were subjected to tensile test at room temperature, impact test in the temperature range 1000–1200°C (Figure 10.14), and to stress–rupture test under standard conditions (Table 10.14).

It can be seen that ultrasonic treatment induced no significant changes in strength characteristics at room temperature and only slightly improved the stress-rupture strength of both alloys (Table 10.14). It

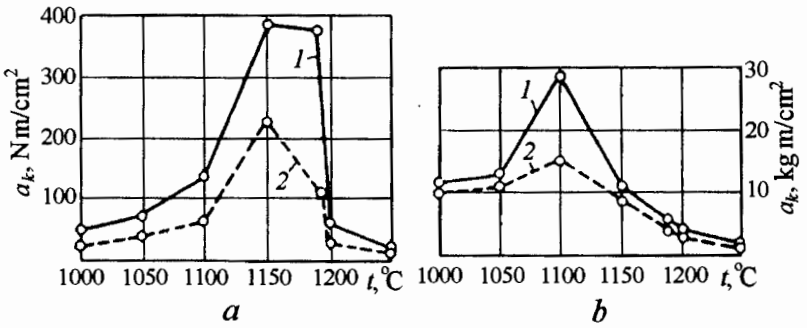

Figure 10.14. Toughness of (*a*) CrNi56WMoCoAl and (*b*) CrNi51WMoTiAlCoVB alloys at working temperatures: (*1*) control ingot, (*2*) ultrasonically solidified ingot.

Table 10.14 Effect of ultrasound on the mechanical properties of as-worked nickel-based superalloys.

Alloy grade	Ultrasonic treatment	Testing temperature, °C	UTS, MPa	YS 0.2 offset, MPa	Elongation, %	Area reduction, %	Stress-rupture strength, *h*		
							900°C, 270 MPa	900°C, 280 MPa	940°C, 220 MPa
CrNi56WMoCoAl	No	20	1290	910	14	14	–	–	–
	Yes	20	1300	920	14	16	–	–	–
	No	900	760	–	10	15	90	–	–
	Yes	900	800	–	10	15	111	–	–
CrNi51WMoTiAlCoVB	No	20	960	760	8	11	–	–	–
	Yes	20	1110	760	8	9	–	–	–
	No	950	600	–	10	11	–	93	75
	Yes	950	630	–	15	16	–	108	75

should be noted that these characteristics for control and ultrasonically treated ingots were close to the standard quality of these alloys produced industrially.

Ultrasonically treated CrNi51WMoTiAlCoVB alloy showed better ductility characteristics, elongation (1.5-fold), and area reduction (2-fold) than control specimen.

Ultrasound enhanced twofold the toughness of CrNi56WMoCoAl and CrNi51WMoTiAlCoVB alloys at temperatures of hot machining.

In work [74], noncorrodable Ni-based alloys Cr15Ni65Mo16Nb and Ni70Mo27W were studied. Ultrasonic irradiation was found to refine their structure and improve their ductility at both room and deformation temperatures.

10.3 Zone Refining Processes

The present-day technology often needs crystals of a specified chemical composition and crystalline perfection. This primarily pertains to the production of monocrystals.

Analysis of ultrasonically induced phenomena in molten and solidifying metals shows that ultrasonic vibrations modify the properties of melts, cause their mixing, and affect the form of crystallization front. All this may play a role in the processes of crystal growth and zonal refining.

The influence of ultrasound on the above processes was the subject of research in a number of works [75–84].

In particular, K. B. Yurkevich [76, 77] studied the zonal refining of zinc (the initial concentration of cadmium was 3.6×10^{-3} and 2.8×10^{-4} mass %) and tellurium (the initial concentrations of copper and selenium were 3×10^{-5} and 4×10^{-3} mass %, respectively).

The method of ultrasonic treatment used by the authors involved a direct transmission of vibrations to a molten zone. This method offers some advantages, such as a favorable influence on the crystallization front and boundary layer, vigorous melt mixing, etc. At the same time, special requirements are imposed, in this case, on the radiator material, which must be refractory and chemically inert with respect to metal melts.

Vibrations at 44 kHz were used. The ingots were subjected to zonal refining in an ultrasonic field of various intensities using a setup presented in Figure 10.15.

High-Intensity Ultrasonics
Theory and Industrial Applications

Oleg V. Abramov
Kurnakov Institute of General and Inorganic Chemistry, Moscow, Russia

This book presents a comprehensive description of the theory and physics of high-intensity ultrasound, as well as dealing with a wide range of problems associated with the industrial applications of ultrasound, mainly in the areas of metallurgy and mineral processing.

The book is divided into three sections, with Part I introducing the reader to the theory and physics of high-intensity ultrasound. Topics in this section include the propagation of ultrasound in liquid media and related nonlinear phenomena, metal crystallization in an ultrasonic field, ultrasound propagation in solids, alterations in dislocational structure, and ultrasonic effects on solidified metal.

In Part II the design of ultrasonic generators, mechanoacoustic radiators and other vibrational systems is considered, as well as the control of acoustic parameters when vibrations are passed into a processed medium.

Part III describes problems associated with various uses of high-intensity ultrasound in metallurgy, for example ore dressing or producing powders and cast composites. The applications of high-intensity ultrasound for metal shaping, thermal and thermochemical treatment, welding, cutting, refining, and surface hardening are also discussed here.

This comprehensive monograph provides an invaluable source of information, which has been largely unavailable in the West until now. The author is very well known and respected internationally within the field of ultrasonics.

Titles of Related Interest

Sonochemistry and Cavitation, *M.A. Margulis*
Ultrasonic Treatment of Light Alloy Melts, *G.I. Eskin*

ISBN: 90-5699-041-1

ISBN 90-5699-041-1
9 789056 990411

Gordon and Breach Science Publishers Australia • Canada
China • France • Germany • India • Japan • Luxembourg • Malaysia
The Netherlands • Russia • Singapore • Switzerland

Amsteldijk 166
1st Floor
1079 LH Amsterdam
The Netherlands

British Library Cataloguing in Publication Data

Abramov, O.V. (Oleg Vladimirovich)
High-intensity ultrasonics : theory and industrial applications
1. Ultrasonic waves - Industrial applications
I. Title
620.2'8

ISBN 90-5699-041-1

CONTEN

Preface

Introduct

I. Phys

1. Low-A
1.1. Harm
1.2. Elasti
1.3. Elasti
1.4. Absor

2. The Pr
Fluids
2.1. Absor
Liquid
2.2. Ultras
2.3. Acoust
2.4. Radiat

3. The Pr
Solids
3.1. Amplit
3.2. Ultras
3.3. Mecha
3.4. Diffusi

4. Nonlin
4.1. Free S
4.2. The M
4.3. Ultras

CONTENTS

Preface ix

Introduction 1

I. Physical Aspects of Ultrasonics 7

1. Low-Amplitude Vibrations and Waves 8
1.1. Harmonic Oscillator 8
1.2. Elastic Waves in Fluids 20
1.3. Elastic Waves in Solids 39
1.4. Absorption of Ultrasonic Waves in Fluids and Solids 52

2. The Propagation of High-Intensity Ultrasonics in Fluids 67
2.1. Absorption of Finite-Amplitude Ultrasonic Waves in Liquids 68
2.2. Ultrasonic Cavitation 80
2.3. Acoustic Streaming 124
2.4. Radiation Pressure 150

3. The Propagation of High-Intensity Ultrasonics in Solids 161
3.1. Amplitude-Dependent Dislocational Internal Friction 161
3.2. Ultrasonically Induced Structural Changes in Solids 174
3.3. Mechanical Properties of Ultrasonically Treated Metals 201
3.4. Diffusion in Ultrasonic Field 223

4. Nonlinear Effects at Interfaces in Fluids 237
4.1. Free Surface in Liquids - Atomization Process 237
4.2. The Mechanism of Ultrasonic Degassing of Liquids 264
4.3. Ultrasonic Emulsification 276

5. Nonlinear Effects at Liquid-Solid and Solid-Solid Interfaces **287**
5.1. Liquid-Solid Interface 287
5.2. Ultrasonically Induced Phenomena at the Solid-Solid Interface 353

II. Ultrasonic Technology **369**

6. Sources of Ultrasonic Energy **369**
6.1. Power Supplies for Ultrasonic Transducers 371
6.2. Mechanoacoustic Transducers 378
6.3. Magnetostrictive Transducers 383
6.4. Piezoceramic Transducers 403

7. Ultrasonic Stacks **413**
7.1. Vibrations in Finite-Size Solids, Cylindrical Sonotrodes 413
7.2. Design Principles of More Complex Sonotrodes 436
7.3. Designing of Ultrasonic Stacks 456

8. Measurement of Acoustic Parameters **463**
8.1. Measurement of Energy Exchange between Oscillator and Transducer 464
8.2. Measurement of Vibration Parameters of Ultrasonic Stacks 472
8.3. Measurement of Vibration Parameters in Loads 481

III. Industrial Applications of High-Intensity Ultrasound **487**

9. Ultrasound in Raw Mineral Dressing **489**
9.1. Flotation and Emulsification of Flotation Reagents 490
9.2. Ultrasonic Disintegration of Minerals and Adhered Surface Films 497
9.3. Application of Ultrasound for Defrothing and Dehydration of Ore Concentrates 503
9.4. Ultrasound in Hydrometallurgy 506

10.
10.1
10.2
10.3
10.4
10.5

11.
11.1
11.2
11.3
11.4
11.5
11.6
11.7
11.8
11.9
11.1
11.1

Co

Ind

10. High-Intensity Ultrasound in Pyrometallurgy **515**
10.1. Ultrasonic Refinement of Melts 515
10.2. Structural Modification of Solidifying Metals 523
10.3. Zone Refining Processes 552
10.4. Ultrasound in Production of Cast Composites 559
10.5. Production of Powders by Ultrasonic Atomization of Melts 570

11. Materials Processing **587**
11.1. Ultrasound in Metalworking 587
11.2. Ultrasound in Heat and Chemical Treatment Processes 594
11.3. Ultrasonic Welding 604
11.4. Ultrasonic Contact and Arc Welding 613
11.5. Ultrasound in Plating Processes 626
11.6. Fatigue Testing at Ultrasonic Frequencies 632
11.7. Ultrasonic Machining 637
11.8. Ultrasonic Surface Treatment 644
11.9. Application of Ultrasound in Electrochemistry 650
11.10. Ultrasonic Impregnation 652
11.11. Ultrasonic Cleaning 656

Conclusion **683**

Index **685**